DECEMBER 1974 MATT-1099

NUMERICAL STUDY OF THE MAGNETOHYDRODYNAMIC SPECTRA IN TOKAMAKS USING GALERKIN'S METHOD

BY

R. L. DEWAR, J. M. GREENE,
R. C. GRIMM AND J. L. JOHNSON

PLASMA PHYSICS LABORATORY

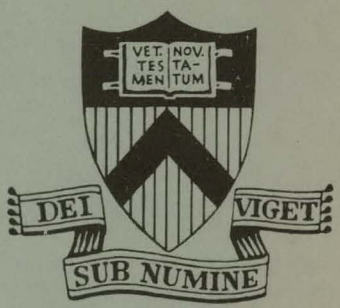

PRINCETON UNIVERSITY
PRINCETON, NEW JERSEY

This work was supported by U. S. Atomic Energy Commission Contract AT(11-1)-3073. Reproduction, translation, publication, use, and disposal, in whole or in part, by or for the United States Government is permitted.

DISCLAIMER

Numerical Study of the Magnetohydrodynamic Spectra in Tokamaks Using Galerkin's Method

R. L. Dewar‡, J. M. Greene,

R. C. Grimm, and J. L. Johnson+

Princeton University

Plasma Physics Laboratory

Princeton, New Jersey

‡Now at the Australian National University, Canberra, A.C.T., Australia.

+On loan from Westinghouse Research Laboratories.

Submitted:

32 pages of manuscript including references
3 tables
1 page of figure captions
2 pages of symbols
4 figures

Send galley proofs to:

J. L. Johnson
Princeton University Plasma Physics Laboratory
P. O. Box 451
Princeton, New Jersey 08540

Running Title

MHD SPECTRA IN TOKAMAKS

ABSTRACT

A computational technique is described for determining the ideal magnetohydrodynamic spectrum and its associated eigenfunctions. The method is suitable for axisymmetric toroidally confined plasmas with arbitrary cross sections. Using the special case of a long, straight, elliptical plasma column with low pressure and uniform axial current where analytic results are available, a study is made of the efficacy of two different choices of expansion functions. The use of a finite-element representation, keeping only a small number of terms, is shown to provide a good description of the system.

I. INTRODUCTION

Because of the renewed interest in tokamak configurations with noncircular cross sections, it is essential that computational techniques be developed with which one can study the magnetohydrodynamic stability properties of the system. Although several such programs have been written [1-9] and have shown promise for the study of specific configurations, it seems appropriate and indeed probably necessary for low-pressure systems to construct one in which the coordinate system is chosen to conform to the physical system. Here we describe such a program and present a specific application to a simple configuration where analytic results are available.[10] This provides an excellent test for comparing different computational procedures against exact results. Further, it provides understanding of the spectrum for a system in which the coupling is relatively complicated.

In Section II we formulate the model problem with sufficient generality that it can be applied to nearly arbitrary axisymmetric configurations. After posing the variational problem we introduce our coordinate system and describe how we project the displacement vector. We then discuss our choices of expansion functions which reduce the problem to one of matrix diagonalization.

In Section III we restrict ourselves to the special case of a long, straight, uniform axial current carrying, low pressure plasma column with an elliptic cross section, embedded in a vacuum. This provides a reasonably good representation of a tokamak. We describe the equilibrium configuration and evaluate expressions for the matrix elements. We compare finite-element with Fourier-Bessel expansions for this model.

The nature of the magnetohydrodynamic spectrum has been the subject of considerable recent interest,[11-14] both because of its usefulness in understanding the instability problem and because of its relevance to the problem of heating a plasma. One application of a code such as this is to study this spectrum. Such work is also useful, in the context of this paper, because it provides a good measure of the efficacy of different techniques. For this reason we provide in Section IV a discussion of the behavior near a singular surface of the eigenfunctions associated with the continuous spectrum.

We present some results for this model in Section V. We study the rate of convergence of the eigenvalues as a function of the number of expansion functions for both Fourier-Bessel and finite-element expansion functions. We also investigate how well the two techniques describe the behavior of an eigenfunction of the continuous spectrum near the singular surface.

II. FORMULATION

The problem of determining the magnetohydrodynamic spectrum of toroidal systems can be posed as that of finding estimates of the eigenvalues ω^2 and eigenfunctions $\vec{\xi}$ that make the Lagrangian

$$L = \omega^2 K\ (\vec{\xi}^*, \vec{\xi}) - \delta W(\vec{\xi}^*, \vec{\xi}) \qquad (1)$$

stationary with respect to variations of ξ. Here $\mathrm{Re}[\vec{\xi}(\vec{r})\ \exp\ (-i\omega t)]$ is the displacement of a fluid element from its equilibrium position $\vec{r}$, and $\omega^2 K$ and δW are the kinetic and potential energy

functionals: [15]

$$2K = \int_p d\tau\ \rho|\vec{\xi}|^2, \tag{2}$$

$$2\delta W = \int_p d\tau\,[|\vec{Q}-\vec{B}\ \frac{\vec{\xi}\cdot\vec{\nabla}p}{B^2}\ |^2 + \frac{\vec{J}\cdot\vec{B}}{B^2}\vec{B}\times\vec{\xi}^*\cdot\vec{Q}$$

$$-2\ \vec{\xi}\cdot\vec{\nabla}p\ \vec{\xi}^*\cdot\vec{\kappa} + \gamma p|\vec{\nabla}\cdot\vec{\xi}|^2]$$

$$+\int_v d\tau\ |\vec{\nabla}\times\vec{A}|^2,$$

with ρ the plasma density, $\vec{Q} \equiv \vec{\nabla}\times(\vec{\xi}\times\vec{B})$ the perturbed magnetic field, $\vec{\kappa} \equiv (\vec{B}/B).\vec{\nabla}(\vec{B}/B)$ the local magnetic field line curvature, γ the ratio of specific heats, and $\vec{A}$ the perturbed vector potential in the vacuum region. The admissible variational functions are those for which the displacement has a finite kinetic energy norm and the normal component of the perturbed magnetic field is continous at the plasma-vacuum interface and vanishes at the vacuum wall.

We adopt the Galerkin method: [16] $\vec{\xi}$ is appeoximated by $\vec{\xi}^{(M)}$, a linear superposition of M linearly independent expansion functions $\vec{\Phi}^{(M)}_m$, viz.,

$$\vec{\xi}^{(M)} = \sum_{m=1}^{M} a_m^{(M)}\ \vec{\Phi}_m^{(M)}. \tag{4}$$

After substitution of Eq. (4) into Eq. (1), variation with respect to $a_{m'}^{(M)*}$ leads to the matrix eigenvalue problem

$$\sum_{m=1}^{M}\left[\omega^{(M)2} < \Phi_{m'}^{(M)*}|K|\Phi_m^{(M)} > - < \Phi_{m'}^{(M)*}|\delta W|\ \Phi_m^{(M)} >\right] a_m^{(M)} = 0 \tag{5}$$

for $\omega^{(M)2}$ and $a_m^{(M)}$. We assume, without proof, that $\vec{\xi}^{(M)}$ converges to a solution of Eq. (1) in the limit as $M\to\infty$. This is a

reasonable assumption since we know from the work of Mikhlin [17,18] that convergence will certainly hold when δW is positive definite, which it is when the plasma is stable. Note that Rayleigh's principle [15] implies that, if $|\vec{\xi} - \vec{\xi}^{(M)}|$ is $O(\varepsilon)$, then $\omega^2 - \omega^{(M)2}$ is $O(\varepsilon^2)$ where $\varepsilon \to 0$ as $M \to \infty$. This provides little help towards choosing the sets of expansion functions that optimise convergence in a practical sense.

The $\vec{\Phi}^{(M)}$ that give the most rapid convergence are the actual eigenfunctions of the system which, of course, we do not know. An obvious approach is to use the exact analytic eigenfunctions of a simpler but similar physical model. Usually, this leads to a global expansion set: one in which the support of all the $\vec{\Phi}_m^{(M)}$ is the entire plasma volume. This approach has been successfully applied. [1,3,19] There are some objections to this attractive scheme. The first is that it is not very flexible; a considerable amount of effort is required to find a good comparison system. Of special relevance is the treatment of localized modes which occur near singular magnetic surfaces. Since these are poorly represented by global expansions with a relatively small number of terms, they might affect the accuracy of all the modes. A further practical difficulty results from the extensive numerical integration required to evaluate the matrix elements. Since all the integrals extend over the plasma volume and the higher eigenfunctions are generally oscillatory, considerable care must be exercised to avoid a rapid deterioration of numerical accuracy as the set of trial functions is increased.

An alternative way of choosing the $\vec{\Phi}_m^{(M)}$'s is to use a finite-

element expansion: one in which the support of each $\vec{\phi}_m^{(M)}$ is only a small region in the plasma. This approach has also been useful. [2,8,9] At first sight, its most serious drawback appears to be that one is forced to work with large matrices. On the other hand, as the system being studied departs from the comparison system it is by no means clear that more expansion functions are required than in a global expansion set.

Since our interest centers on axially symmetric configurations, it is appropriate to describe the equilibrium magnetic field by

$$\vec{B} = B_o \left[f(\psi) \vec{\nabla} \phi \times \vec{\nabla} \psi + R\, g(\psi) \vec{\nabla}\phi \right]. \tag{6}$$

Here the azimuthal angle ϕ is the ignorable coordinate and the magnetic field lines form surfaces labeled by constant values of ψ. The poloidal flux inside a surface is given by $2\pi B_o \int f d\psi$. The function g associated with the toroidal field must depend on ψ alone so that the current lies in the magnetic surfaces.

It is obvious that ϕ should be used as a coordinate.

Since current can flow freely along field lines, and fluid can not cross them, it is clear that plasma behavior is quite anisotropic. Mathematically, our equations are higher order in derivatives within magnetic surfaces than in derivatives across them. To represent this with good numerical accuracy, it seems necessary to use ψ as a coordinate. In this system the plasma-vacuum interface is a coordinate surface. This makes it easy to use Green's function techniques to express the extremized contribution to δW from the vacuum region outside the plasma in terms of the components of an arbitrary $\vec{\xi}\cdot\vec{\nabla}\psi$ on this surface.

It is not clear what one should choose to label the third coordinate. One obvious choice would be to construct an orthogonal system so as to simplify the analysis. Unfortunately, this formal simplification doesn't guarantee practical improvement. A second possible choice would be to determine the coordinate θ in such a way that the magnetic field lines are straight, so that

$$\vec{B}\cdot\vec{\nabla} = \vec{B}\cdot\vec{\nabla}\theta \quad (\partial/\partial\,\theta + q(\psi)\ \partial/\partial\phi)$$

since this particular operator enters the calculation in many places. This choice makes the Jacobian

$$J \equiv (\vec{\nabla}\psi \times \vec{\nabla}\theta\cdot\vec{\nabla}\phi)^{-1} = \frac{X^2}{4\pi^2}\int_p \frac{d\tau}{X^2}\ , \tag{7}$$

where X is the distance from the major axis. Here we normalize ψ to unity on the plasma-vacuum interface. A third possibility would be to choose θ to make the Jacobian a function of ψ alone. We adopt the idea associated with Eq. (7) since it provides a natural representation of the physics associated with behavior near a closed magnetic field line and has proven useful for many applications. For the special configuration discussed in Section III, this also makes J a constant.

We now consider the decomposition of the displacement vector in the plasma region. Keeping in mind the fact that the Lagrangian is diagonalized by the normal modes of the physical system, we should choose components of the perturbations that represent the polarizations of the various modes, at least in the low pressure, long wave length limit that is reasonable for present day devices. This is also likely to be the most troublesome regime, since the range between the highest and

lowest eigenvalues is most exaggerated here. Indeed, the frequency range spans many orders of magnitude. The lowest frequency, or sound, modes consist of flow along the magnetic field lines. The next branch, that of shear-Alfven waves, has a divergencefree motion perpendicular to the field. The fast magnetosonic mode is primarily due to this perpendicular compressibility. Since the frequencies of these different branches can be widely separated, it is important to select the representation so that evaluation of the spectrum does not rely on cancellation of large terms for its accurate calculation. The sound waves are well treated by the projection

$$\vec{\xi} = (J\xi_\psi/gR^2B_o)\,\vec{\nabla}\theta \times \vec{B} + i(J\xi_s/gR^2B_o)\,\vec{B} \times \vec{\nabla}\psi + i(\tau/B_o)\vec{B}, \tag{8}$$

while, at least in the long wavelength limit, the shear Alfvén and compressional branches are decoupled by the transformation

$$\xi_\psi = \delta - 2\pi\, i\, \partial\zeta/\partial\theta,$$
$$\xi_s = 2\pi\, \partial\zeta/\partial\psi. \tag{9}$$

We next consider the treatment of the vacuum region. We see from Eqs. (1) and (3) that the Lagrangian L is extremized if $\vec{\nabla} \times (\vec{\nabla} \times \vec{A}) = 0$, or $\vec{\nabla} \times \vec{A} = \vec{\nabla}\chi$. Taking the divergence of this latter expression, we find that

$$\nabla^2\chi = 0. \tag{10}$$

Further, multiplying Eq. (10) by χ and integrating over the vacuum region, we see that

$$2\delta W_v = -2\pi \int_0^{2\pi} d\theta J \chi^* \vec{\nabla} \chi \cdot \vec{\nabla}\psi \qquad (11)$$

evaluated over the plasma-vacuum interface. The contribution to δW from the outer wall vanishes because the normal component of the perturbed field must be zero there. Since this component of the perturbed field is equal to $\vec{Q}\cdot\vec{\nabla}\psi/|\vec{\nabla}\psi|^2$ on the interface, the vacuum problem reduces to one of evaluating χ (θ) on this boundary. This is accomplished by writing a Green's function solution of Eq. (10) which enables us to determine χ in terms of Q_ψ on the interface. If toroidal effects are negligible, this reduces to

$$\chi(s) = \frac{1}{\pi} \oint dt \left[\chi(t) \frac{\partial K_o(kr)}{\partial n} - K_o(kr) \frac{\partial \chi(t)}{\partial n}\right], \qquad (12)$$

where $r \equiv |\vec{r}(s) - \vec{r}(t)|$, $\partial/\partial n$ is the normal derivative, and the contour is taken over both the plasma-vacuum interface and an arbitrarily placed conducting wall. Marder[20] used this technique for straight systems with very long periodicity length such that the Bessel function K_o could be represented by a log function.

Now that we have chosen our coordinates and described the polarizations of our perturbations, it is appropriate to continue the discussion of the choice of the expansion functions $\vec{\Phi}_m^{(M)}$. It is convenient to use Fourier series in θ and ϕ.

$$\vec{\xi}(\vec{r}) = \sum_{\ell,n} \vec{\xi}_{\ell,n}(\psi) \exp i(\ell\theta - n\Phi). \qquad (13)$$

The different terms in n decouple and we can drop this subscript accordingly. Obviously, we can not expect decoupling in θ. It is useful to note, however, that if the configuration possesses sufficient symmetry, modes with even and odd values of ℓ do not

couple and we can treat them separately. In the numerical work it is essential to truncate the series in ℓ.

In this paper we discuss two ways of representing the ψ dependence. We choose for our global expansion functions the eigenmodes of a straight plasma column with circular cross section and uniform current and density profiles. Thus we set

$$\zeta_\ell(\psi) = \sum_{m=0}^{M} \zeta_{\ell,m} \Phi^{(M)}_{\ell,m}(\psi), \tag{14}$$

where

$$\Phi^{(M)}_{\ell,0} = \psi^{|\ell|/2},$$

$$\Phi^{(M)}_{\ell,m} = J_\ell(j_{\ell,m}\psi^{1/2}), \qquad m = 1, 2, \cdots, M \tag{15}$$

with $j_{\ell,m}$ the m'th root of J_ℓ, and with similar expressions for δ_ℓ and τ_ℓ. The Bessel functions are a complete set of functions that vanish on the boundary $\psi=1$. In a circular pinch with constant axial current and density, they can represent the infinite set of degenerate Alfvén modes. The algebraic term must be added to complete the representation of functions with arbitrary boundary values. This term is the eigenfunction for a kink mode in a circular system. We must omit the $\zeta_{0,0}$ term which would not contribute to the kinetic or potential energy.

We use for our finite-element approach a tent function expansion

$$\Phi^{(M)}_{\ell,m} = MT_\ell(\psi)\,[(\psi-\psi_{m-1})H(\psi-\psi_{m-1})H(\psi_m-\psi)$$

$$-(\psi-\psi_{m+1})H(\psi-\psi_m)H(\psi_{m+1}-\psi)]. \tag{16}$$

The Heaviside functions $H(p) \equiv (p+|p|)/2p$ make the Φ's vanish except between the nodal points ψ_{m-1} and ψ_{m+1}, where $\psi_m \equiv m/M$ The function $T_\ell(\psi)$ is one when ℓ is even and $\psi^{1/2}$ when ℓ is odd. This function is introduced for the odd modes because the analytic work[10] indicates that $\zeta_\ell(\psi) = O(\psi^{|\ell|/2})$ as $\psi \to 0$. Thus it improves the representation. It is necessary to set $\zeta_{\ell,0}$ and $\delta_{\ell,0}$ to zero to avoid an infinite kinetic energy. An elegant way of removing the singularity in K resulting from the addition of an arbitrary constant to ζ is to add the projection matrix

$$P(\Phi^{(M)*}_{\ell',m'}, \Phi^{(M)}_{\ell,m}) \equiv \delta_{\ell',0}\,\delta_{\ell,0} \tag{17}$$

to $K(\Phi^{(M)*}_{\ell',m'}, \Phi^{(M)}_{\ell,m})$. This projects onto the one-dimensional subspace spanned by the ζ= constant solution and, thus, does not affect the true eigenmodes of the system. It makes the problem well defined by replacing the kinetic energy with a positive definite matrix. It introduces a spurious eigenmode at $\omega^2 = 0$ which provides a check on the numerical accuracy of the calculation. Equation (16) provides a good basis for expansion of the ζ_ℓ's and δ_ℓ's in Eq. (14). However, it is useful to introduce another set of expansion functions for the τ_ℓ's. We chose it to be

$$\Phi^{(M)}_{\ell,m} = H(\psi-\psi_{m-1})H(\psi_m-\psi). \tag{18}$$

This is a reasonable choice because, unlike ζ_ℓ and δ_ℓ, there are no ψ derivatives of τ_ℓ. As with many numerical problems, one

can either use lowest-order interpolations or higher-order schemes. We have chosen the class with the lowest continuity properties consistent with a finite kinetic energy norm.

When either the global or the local expansion scheme is substituted into Eq. (1), we are led to the matrix problem of Eq. (5). One might hope that when global expansion techniques are employed the matrices can be kept small such that standard matrix eigenvalue schemes are satisfactory. The matrices can be large, but sparse, when local expansions are made. Some progress has been made towards developing efficient techniques for obtaining the eigenvalues and eigenfunctions of large, sparse systems by Lagrangian reduction.[21]

III. APPLICATION

Our discussion has been very general until now. In order to be specific, we restrict consideration to a special case which is amenable to analytic treatment[10] and is therefore especially useful for testing the efficacy of different types of expansion functions. Results obtained from a generalization of this model to include the effects of pressure gradients and finite axial length are forthcoming.[22]

A. Model

We consider a cylindrical column with an elliptic cross section confined in a uniform axial magnetic field B_z, carrying a uniform axial current J_z, and embedded in a vacuum. For simplicity, we assume that the plasma pressure is negligible, the axial current is small, and the periodicity length L is large.

This is the usual representation of a tokamak configuration to lowest order in the inverse aspect ratio. Thus, we assume that $(p/B_z^2)^{1/2} \sim B_\perp / B_z \sim a/L \equiv \varepsilon << 1$, where a measures the size of the elliptic cross section of the plasma. We set $f(\psi) = b^2a^2LJ_z/4\pi B_o (b^2+a^2)$ and $g(\psi) = 1$. Then, from the condition that $\vec{J} = \vec{\nabla} \times \vec{B}$, we find that, in the usual cartesian coordinates, $\psi = x^2/a^2+y^2/b^2$ inside the plasma. The natural coordinate system (ψ, Θ, z) is given by

$$x = a\psi^{1/2} \cos \Theta, \tag{19}$$
$$y = b\psi^{1/2} \sin \Theta.$$

In this model

$$\vec{B} \cdot \vec{\nabla} = (kB_o/q) [\partial/\partial\Theta + (g/k) \partial/\partial z] \tag{20}$$

and

$$J = baL/4\pi \tag{21}$$

with $k \equiv 2\pi/L$ and the safety factor $q = ba/2f$ a constant throughout the plasma.

Dewar et al.[10] showed that the frequencies of the magnetosonic waves are large, of order ε^{-2}, compared to those associated with kink modes and shear Alfvén waves. We set $\delta_\ell = 0$ to make $\vec{\nabla} \cdot \vec{\xi}_\perp = 0$ and thus eliminate the fast magnetosonic modes. We also take $\tau_\ell = 0$ to remove the sound waves. This reduces Eq. (1) to

$$L = \frac{4\pi^3 B_o^2}{baL\, q^2} \sum_{\ell,\ell'} \left\{ \frac{\omega^2}{\omega_a^2} \int_0^1 d\psi\, \frac{\rho(\psi)}{\rho_o} M\left[\zeta^*_{\ell'}(\psi), \zeta_\ell(\psi)\right] \right.$$

$$- (\ell - nq)(\ell' - nq) \int_0^1 d\psi\, M\left[\zeta^*_{\ell'}(\psi), \zeta_\ell(\psi)\right]$$

$$\left. + \left[\ell(\ell - nq)(b^2 + a^2) - |\ell|\,(\ell - nq)^2\, ba\right] |\zeta_\ell(1)|^2\, \delta_{\ell',\ell} \right\} \qquad (22)$$

with

$$M\left[\zeta^*_{\ell'}(\psi), \zeta_\ell(\psi)\right] \equiv (b^2 + a^2)\left[\psi |\zeta'_\ell(\psi)|^2 + \frac{\ell^2}{4\psi} |\zeta_\ell(\psi)|^2\right] \delta_{\ell',\ell}$$

$$+ \frac{(b^2 - a^2)\psi}{2}\left[\zeta'_\ell(\psi) - \frac{\ell}{2\psi}\zeta_\ell(\psi)\right]\left[\zeta'^*_{\ell'}(\psi) + \frac{\ell'}{2\psi}\zeta^*_{\ell'}(\psi)\right] \delta_{\ell',\ell+2}$$

$$+ \frac{(b^2 - a^2)\psi}{2}\left[\zeta'_\ell(\psi) + \frac{\ell}{2\psi}\zeta_\ell(\psi)\right]\left[\zeta'^*_{\ell'}(\psi) - \frac{\ell'}{2\psi}\zeta^*_{\ell'}(\psi)\right] \delta_{\ell',\ell-2}. \qquad (23)$$

Here $\omega_a^2 \equiv k^2 B_o^2 / \rho_o q^2$, where $\rho_o = \int_o^1 \rho(\psi)\, d\psi$, is a poloidal Alfvén frequency and primes denote derivatives with respect to ψ. The last term in Eq. (22) enters through Eq. (11) which can be evaluated analytically in this model. The problem, then, is to determine the functions $\zeta_\ell(\psi)$ that extremize Eq. (22).

B. Expansion Functions

We first use the global expansion functions defined in Eq. (15). If the plasma density as well as the axial current is uniform inside the plasma, the integrals in Eq. (22) can be evaluated analytically; thus

$$\int_0^1 d\psi \; M\left[\zeta^*_{\ell'}(\psi),\, \zeta_{\ell}(\psi)\right] \equiv \sum_{m,m'} a^*_{\ell',m'}\, \hat{M}_{\ell',m',\ell,m}\, a_{\ell,m} \qquad (24)$$

where

$$\hat{M}_{\ell',m',\ell,m} = \frac{(b^2+a^2)}{4}\left[j^2_{\ell,m}\, J^2_{|\ell|+1}(j_{\ell,m})\, \delta_{m',m}\,(1-\delta_{m,o}) + 2|\ell|\,\delta_{m',o}\,\delta_{m,o}\right]\delta_{\ell',\ell}$$

$$- \frac{(b^2-a^2)}{2}\left\{ \frac{(\ell+1)\, j_{\ell',m'}\, j_{\ell,m}}{(j^2_{\ell',m'} - j^2_{\ell,m})}\, J_{|\ell'|+1}(j_{\ell',m'}) \times J_{|\ell|+1}(j_{\ell,m})\,(1-\delta_{m',o})\,(1-\delta_{m,o}) \right.$$

$$+ \frac{2|\ell'||\ell+1|}{j_{\ell,m}}\, H(\ell+1)\, J_{|\ell|+1}(j_{\ell,m})\,\delta_{m',o}\,(1-\delta_{m,o})$$

$$+ \frac{2(-1)^{\ell'}|\ell||\ell+1|}{j_{\ell',m'}}\, H(-\ell-1)\, J_{|\ell'|+1}(j_{\ell',m'})\,(1-\delta_{m',o})\,\delta_{m,o}$$

$$\left. + \left[\delta_{m,o} + \frac{j^2_{1,m}}{4} J^2_0(j_{1,m})\,(1-\delta_{m,o})\right]\delta_{m',m}\,\delta_{\ell,-1} \right\}\delta_{\ell',\ell+2}$$

$$- \frac{(b^2-a^2)}{2}\left\{ \frac{(\ell'+1)\, j_{\ell',m'}\, j_{\ell,m}}{(j^2_{\ell,m} - j^2_{\ell',m'})}\, J_{|\ell'|+1}(j_{\ell',m'}) \times J_{|\ell|+1}(j_{\ell,m})\,(1-\delta_{m',o})\,(1-\delta_{m,o}) \right.$$

$$+ \frac{2|\ell'+1||\ell|}{j_{\ell',m'}}\, H(\ell'+1)\, J_{|\ell'|+1}(j_{\ell',m'})\,(1-\delta_{m',o})\,\delta_{m,o}$$

$$+ \frac{2(-1)^{\ell}|\ell'||\ell'+1|}{j_{\ell,m}}\, H(-\ell'-1)\, J_{|\ell|+1}(j_{\ell,m})\,\delta_{m',o}\,(1-\delta_{m,o})$$

$$\left. + \left[\delta_{m,o} + \frac{j^2_{1,m}}{4} J^2_0(j_{1,m})\,(1-\delta_{m,o})\right]\delta_{m',m}\,\delta_{\ell',-1} \right\}\delta_{\ell',\ell-2} \qquad (25)$$

with $H(p) \equiv (p+|p|)/2p$. It is easily seen that $\hat{M}_{o,o,o,o}$ is zero, corresponding, as previously noted, to the fact that one can add an arbitrary constant to ζ in Eq. (9) without changing $\vec{\xi}$. Analytic expressions for the kinetic energy term K cannot be found if the density varies and the integrals must be evaluated numerically.

Introducing the expansion functions of Eq. (16) leads to matrix elements with

$$\hat{M}_{\ell',m',\ell,m} = \frac{(b^2+a^2)}{4}\left(\ell^2 P^{(1)}_{m',m} + 4\,P^{(3)}_{m',m}\right)\delta_{\ell',\ell}$$
$$-\frac{(b^2-a^2)}{8}\left(\ell'\ell P^{(1)}_{m',m} - 2\ell' P^{(2)}_{m,m'} + 2\ell P^{(2)}_{m',m} - 4\,P^{(3)}_{m',m}\right)\delta_{\ell',\ell+2}$$
$$-\frac{(b^2-a^2)}{8}\left(\ell'\ell P^{(1)}_{m',m} + 2\ell' P^{(2)}_{m,m'} - 2\ell P^{(2)}_{m',m} - 4P^{(3)}_{m',m}\right)\delta_{\ell',\ell-2} \tag{26}$$

for even ℓ, with

$$P^{(1)}_{m',m} \equiv \int_0^1 \frac{d\psi}{\psi}\,\Phi^{*}_{\ell',m'}(\psi)\,\Phi_{\ell,m}(\psi)$$
$$= \left\{\left[-2m+(m-1)^2 \ln\left(m/(m-1)\right) + (m+1)^2 \ln\left((m+1)/m\right)\right]\delta_{m',m}\right.$$
$$+\left[\frac{1}{2}(2m+1) - m(m+1)\ln\left((m+1)/m\right)\right]\delta_{m',m+1}$$
$$\left.+\left[\frac{1}{2}(2m-1) - m(m-1)\ln\left(m/(m-1)\right)\right]\delta_{m',m-1}\right\}$$
$$\times (1-\delta_{m',o}\,\delta_{m,o})\,(1-\delta_{m',M}\,\delta_{m,M})$$
$$+\left[\frac{1}{2}(3-2M) + (M-1)^2 \ln\left(M/(M-1)\right)\right]\delta_{m',M}\,\delta_{m,M} \tag{27}$$

[Should one wish to include the trivial perturbation associated with Eq. (17), it is useful to note that $P^{(1)}_{m',m}$ with m' or m zero does not need consideration since it is always multiplied by $\ell'\ell$ in Eq. (26).],

$$P^{(2)}_{m',m} = \int_0^1 d\psi \Phi^{'}_{\ell',m'}(\psi)\ \Phi_{\ell,m}(\psi)$$

$$= 1/2\ (\delta_{m',m+1} - \delta_{m',m-1})\ (1-\delta_{m',o}\ \delta_{m,o})\ (1-\delta_{m',M}\ \delta_{m,M})$$

$$- 1/2\ \delta_{m',o}\ \delta_{m,o} + 1/2\ \delta_{m',M}\ \delta_{m,M}) \qquad (28)$$

and

$$P^{(3)}_{m',m} = \int_0^1 d\psi\psi\Phi^{'}_{\ell',m'}(\psi)\ \Phi^{'}_{\ell,m}(\psi)$$

$$= \left[2m\delta_{m',m} - 1/2\ (2m-1)\delta_{m',m+1} - 1/2\ (2m+1)\ \delta_{m',m-1} \right]$$

$$\times\ (1-\delta_{m',o}\ \delta_{m,o})\ (1-\delta_{m',M}\ \delta_{m,M})$$

$$+ 1/2\ \delta_{m',o}\ \delta_{m,o} + 1/2\ (2M-1)\ \delta_{m',M}\ \delta_{m,M}. \qquad (29)$$

For odd ℓ

$$\hat{M}_{\ell',m',\ell,m} = \frac{(b^2+a^2)}{4} \left[(\ell^2+1)\ Q^{(1)}_{m',m} + 2Q^{(2)}_{m',m} + 2Q^{(2)}_{m,m'} + 4Q^{(3)}_{m',m} \right] \delta_{\ell',\ell}$$

$$- \frac{(b^2-a^2)}{8} \left[(\ell'+1)\ (\ell-1)\ Q^{(1)}_{m',m} + 2\ (\ell-1)\ Q^{(2)}_{m',m} - 2(\ell'+1)\ Q^{(2)}_{m,m'} - 4\ Q^{(3)}_{m',m} \right] \delta_{\ell',\ell+2}$$

$$- \frac{(b^2-a^2)}{8} \left[(\ell'-1)\ (\ell+1)\ Q^{(1)}_{m',m} - 2(\ell+1)\ Q^{(2)}_{m',m} + 2(\ell'-1)\ Q^{(2)}_{m,m'} - 4\ Q^{(3)}_{m',m} \right] \delta_{\ell',\ell-2}, \qquad (30)$$

with

$$Q^{(1)}_{m',m} = \int_0^1 \frac{d\psi}{\psi}\, \Phi^{*}_{\ell',m'}(\psi)\, \Phi_{\ell,m}(\psi)$$

$$= \frac{1}{6M}\Big\{ (4\delta_{m',m} + \delta_{m',m+1} + \delta_{m',m-1})\,(1-\delta_{m',0}\,\delta_{m,0})$$

$$\times\,(1-\delta_{m',M}\,\delta_{m,M}) + 2\delta_{m',0}\,\delta_{m,0} + 2\delta_{m',M}\,\delta_{m,M}\Big\}, \qquad (31)$$

$$Q^{(2)}_{m',m} = \int_0^1 \psi^{1/2}\, d\psi \Big[\, d(\psi^{-1/2}\,\Phi^{*}_{\ell',m'}(\psi))/d\psi \,\Big]\, \Phi_{\ell,m}(\psi)$$

$$= -\frac{1}{6M}\Big\{ \Big[2\delta_{m,m'} + (3m+1)\,\delta_{m',m+1} - (3m-1)\,\delta_{m',m-1} \Big]$$

$$\times\,(1-\delta_{m',0}\,\delta_{m,0})\,(1-\delta_{m',M}\,\delta_{m,M})$$

$$+ \delta_{m',0}\,\delta_{m,0} - (3M-1)\,\delta_{m',M}\,\delta_{m,M}\Big\}, \qquad (32)$$

and

$$Q^{(3)}_{m',m} = \int_0^1 \psi^2 d\psi\, \frac{d(\psi^{-1/2}\Phi^{*}_{\ell',m'}(\psi))}{d\psi}\, \frac{d(\psi^{-1/2}\Phi_{\ell,m}(\psi))}{d\psi}$$

$$= \frac{1}{3M}\Big[2(3m^2+1)\,\delta_{m',m} - (3m^2+3m+1)\,\delta_{m',m+1} - (3m^2-3m+1)\,\delta_{m',m-1} \Big]$$

$$\times\,(1-\delta_{m',0}\,\delta_{m,0})\,(1-\delta_{m',M}\,\delta_{m,M})$$

$$+ \delta_{m',0}\,\delta_{m,0} + (3M^2-3M+1)\,\delta_{m',M}\,\delta_{m,M}\,. \qquad (33)$$

IV SPECTRAL PROPERTIES

Although our major interest lies in determining the nature of the unstable modes that are possible in a specific configuration, it is worthwhile to investigate the full spectrum of the system.

Analytic determination of the spectrum is quite difficult to accomplish in general. However, considerable understanding of the nature and number of continuous and discrete spectra that are present can be obtained from a study of special cases. Here we sketch such a calculation to indicate what should be expected.

Continuous spectra are characterized by eigenfunctions having singular behavior somewhere inside the plasma. For example, if the matrix associated with terms with the highest derivative with respect to ψ in the Lagrangian has a vanishing determinant on some surface inside the plasma, then the eigenfuctions can have a local [ln $(\psi-\psi_o)$ + constant] behavior. At such points the constant can have an arbitrary finite discontinuity. This provides the possibility of satisfying the boundary conditions for a band of eigenvalues and leads to a continuous spectrum.

For definiteness, consider the model treated in Sect. III. We see from Eq. (22), or from Eq. (25) of Dewar et al.,[10] that the set of Euler-Lagrange equations that makes the Lagrangian, Eq. (1), stationary can be written in the form

$$L(\zeta) \equiv T\zeta''(\psi) + (T'+T/\psi + W/\psi)\,\zeta'(\psi)$$

$$+ (W'/2\psi + X/4\psi^2)\,\zeta(\psi) = 0, \qquad (34)$$

where primes denote derivatives with respect to ψ, T, W, and X are the infinite tridiagonal matrices

$$T(\psi) \equiv (G_{\ell-1},\ 2F_\ell \cosh 2\mu_o,\ G_{\ell+1}),$$

$$W(\psi) \equiv \left(-(\ell-1)\,G_{\ell-1},\ 0,\ (\ell+1)\,G_{\ell+1}\right),$$

$$X(\psi) \equiv \Big(2\psi G'_{\ell-1} + \ell(\ell-2)\, G_{\ell-1}, - 2\ell^2 F_\ell \cosh 2\mu_o,$$

$$2\psi G'_{\ell+1} + \ell(\ell+2)\, G_{\ell+1} \Big), \qquad (35)$$

and ζ is the vector $\{\zeta_\ell\}$ with ℓ odd.

Clearly, the set of modes with ℓ even can be treated similarly. As in the earlier work,[10]

$$F_\ell \equiv \left[(\ell - nq)^2 - \rho^2/\rho_o \omega_a{}^2 \right],$$

$$G_\ell \equiv \left[(\ell+1-nq)\,(\ell-1-nq) - \rho\omega^2/\rho_o \omega_a{}^2 \right],$$

and

$$\cosh 2\mu_o = (b^2+a^2) \,/\, (b^2-a^2).$$

Note that T and X are symmetric matrices and W is antisymmetric. We approximate this system by working with finite matrices of order 2N+1.

We choose a $\psi=\psi_s$ and ω^2 such that the determinant of $T_o \equiv T(\psi_s)$ is zero. This eigenvalue problem for ω^2 is equivalent to the eigenvalue problem

$$\left[\left(\frac{\partial}{\partial\Theta} - inq\right) |\vec{\nabla}\psi|^2 \left(\frac{\partial}{\partial\Theta} - inq\right) + \frac{\rho\omega^2}{\rho_o \omega_a^2} |\vec{\nabla}\psi|^2 \right] \zeta''(\psi_s, \Theta) = 0 \qquad (36)$$

when $|\vec{\nabla}\psi|^2$ is expressed in the ψ,Θ coordinate system of Sect. II. The possible eigenvalues ω^2 form a continuum as ψ_s ranges from 0 to 1.

The system of Eqs. (34) is singular at $y \equiv \psi - \psi_s = 0$, and we seek solutions that vary as y^p. We calculate the eigenvalues and eigenvectors of T_o,

$$T_o\, \xi_k = \lambda_k\, \xi_k, \qquad k = -N, \ldots, N, \qquad (37)$$

and arrange the counting so that λ_o is the nondegenerate vanishing

eigenvalue. For simplicity, we assume that $(\xi_o, T_o' \xi_o) \neq 0$. The modifications of the ensuing discussion that would otherwise be necessary are straightforward but tedious.

Introducing the projection operator

$$(P_o)_{ij} = (\xi_o)_i \ (\xi_o)_j \tag{38}$$

so that

$$P_o \xi_o = \xi_o; \quad P_o \xi_k = 0, \quad k \neq 0,$$

we can express ζ in a series

$$\zeta = \sum_{m=0}^{\infty} \tau_m, \tag{39}$$

where

$$\tau_m = y^{p+m-1} P_o \sigma_m + y^{p+m} (1-P_o) \sigma_m \tag{40}$$

with p to be determined and the σ_m a set of vector constants. Introducing Eq. (40) into Eq. (34) yields

$$L(\tau_m) = y^{p+m-2} H(p+m) \sigma_m + O(y^{p+m-1}) \tag{41}$$

where

$$H(p) = p(p-1) T_o + [(p-1)^2 T_o' + (p-1) W_o/\psi_s] P_o. \tag{42}$$

Thus Eq. (34) is converted, by equating powers of y, into a set of equations for σ_m in terms of σ_n with $n < m$. In order that these equations can be solved successively, it is necessary that H (p) not have a vanishing determinant. This is the case, as can be seen in the representation where T_o is diagonal, because we have assumed that λ_o is not degenerate, $(\xi_o, T_o' \xi_o) \neq 0$, and we can observe that $(\xi_o, W\xi_o) = 0$ since W is antisymmetric.

The equation for σ_o is homogeneous. In order for it to have a solution, the determinant of $H(p)$, which is proportional to $p^{2N}\ (p-1)^{2N+2}$, must vanish. When $p=0$, $H\sigma_o = 0$ has $2N$ independent solutions that can be expressed as

$$\sigma_o = (1 - P_o)\ \upsilon_o \tag{43}$$

where υ_o is an arbitrary vector. When $p=1$, it has $2N+1$ independent solutions

$$\sigma_o = \upsilon_1 \tag{44}$$

with υ_1 arbitrary. The remaining solution for $p=1$ is logarithmic; it can be expressed as

$$\zeta = \bar{\zeta}\ \ln y + \sum_{m=1}^{\infty} \tau_m, \tag{45}$$

where $\bar{\zeta}$ is the particular $p=1$ solution of Eq. (34) for which $\bar{\sigma}_o$ satisfies

$$\frac{\partial H(p)}{\partial p}\Big|_{p=1}\ \bar{\sigma}_o = \left(T_o + \frac{W_o P_o}{\psi_s}\right)\ \bar{\sigma}_o = 0. \tag{46}$$

Thus

$$\zeta = \xi_o\ \ln\ (\psi-\psi_s) + \Theta(1). \tag{47}$$

The natural conditions for matching across the singularity are that the $2N$ $p=0$ solutions, the $2N$ $p=1$ solutions orthogonal to ξ_o, and the logarithmic term should be continuous, while the $p=1$ solution proportional to $\bar{\sigma}_o$ can have an arbitrary jump, since the constant of proportionality may be hidden by the logarithm. This provides an extra freedom and permits ω^2 to be an eigenvalue of Eq. (1) regardless of boundary conditions.

Since the eigenfunction associated with Eq. (47) is dominant near $\psi = \psi_s$, comparison of the behavior of the different components ζ_ℓ (in the Θ decomposition) can provide a strong indication of how well the numerical program determines the eigenfunctions.

It is instructive to note that in this model there is only one continuous spectrum which is associated with the propagation of shear Alfvén waves. The low-pressure assumption has caused the sound branch to coalesce into an infinite degeneracy at $\omega^2=0$, while the incompressibility condition has pushed the discrete fast magnetosonic modes to $\omega^2=\infty$. Another relatively simple model is the diffuse linear pinch, in which the different modes in θ as well as in z decouple. In this case the eigenvalue problem associated with T_o, analogous to Eq. (36), and including the coupling to δ and τ, is

$$\left[(\ell-nq)^2 - \frac{\rho\omega^2}{\rho_o\omega_a^2 g^2} \right] \left[(\ell-nq)^2\Gamma - \frac{\rho\omega^2(1+\Gamma)}{\rho_o\omega_a^2 g^2} \right] \zeta''(\psi_s) = 0 \qquad (48)$$

with $\Gamma \equiv \gamma p/B$. Following the general lines of the above calculation, we see that there are two distinct continuous spectra, one corresponding to each of the two roots of Eq. (48). This is in agreement with the results of Appert *et al.* [23] and of others.[24] We are at present developing programs that will illustrate these continua in more complicated systems.

V. NUMERICAL RESULTS

The computer program as presently operating is applicable to the special case described in Sect. III. Dewar *et al.*[10] reported the results of the study of the spectrum as a function of nq which measures the net axial current inside the plasma for various plasma density distributions. In this paper we concentrate on the convergence properties of the method, comparing eigenvalues and eigenfunctions in discrete and continuous branches of the spectrum for both global and local expansion functions.

We first consider how the eigenvalue ω^2 varies as we increase the number of expansion functions. For constant density elliptical equilibria, the results can be compared directly with analytic solutions, [10] so that this case constitutes a valuable nontrivial test of the numerical method. We consider a system with nq = 1.5 and b/a = 2, such that the configuration is unstable to the $\ell = 2$ kink mode. In Table I we tabulate numerical estimates of the values of ω^2 for several normal modes of the system versus the number of expansion functions. The results of both the Fourier-Bessel expansion of Eqs. (15) and (25) and the finite elements of Eqs. (16), (26), and (30) are given, together with the analytical result. With both expansions convergence to the correct result is rapid, good accuracy being achieved over the entire spectrum considered with very few terms. The rather special mode coupling demonstrated by the analytic calculation for this constant density case enables an exceptionally good representation of the lower Fourier modes, while as more modes couple when we consider higher mode numbers the convergence is understandably slower. Of course truncation of the Fourier series expansion will always lead to somewhat incorrect values for the frequencies of those modes with ℓ-numbers near the limits of the expansion. The number of Fourier elements required will also depend on the value of b/a, and in general this must be determined empirically in much the same manner as M is. The accuracy with which the $\ell = \pm 4$ modes are obtained from this calculation, which used a relatively large value of b/a, gives us reasonable confidence in the efficacy of the Fourier expansion.

With a nonconstant density we lose the particularly convenient decoupling symmetries that lead to the analytic solutions and to the excellent agreement shown in Table I. In Table 2 we compare the convergence of the $\ell = 2$ kink mode for a system with identical parameters to the previous case but with $\rho(\psi) = 1.2 - 0.4\psi$ ———— i.e. a roughly parabolic density profile. Again the convergence is excellent, good accuracy being obtained with six terms in either expansion. The comparison of Table 2 is typical of our experience with runs with different values of b/a, nq, and $\rho(\psi)$; viz, the global expansions show no significant improvement in convergence over the finite-element expansion for the non-localized magnetohydrodynamic modes. As indicated by the analytic work, this result no doubt has its origin in the coupling through ellipticity to highly localized continuous Alfvén modes. As we shall see later, the finite-element expansion gives a far more satisfactory representation of these modes. Since considerably more computation is involved in the Fourier-Bessel expansion than with finite elements for the same number of terms, this comparison indicates that the latter expansion is more desirable.

One feature that emerges from a careful study of the results is that the convergence can not always be described empirically as $O(M^p)$. In any given calculation the value of p necessary to fit the data differs from one mode to another so that extreme care is necessary in trying to extrapolate to exact results.

To show how well the eigenfunctions are approximated we show in Fig. 1 the $\ell = 2$ component of $[\zeta - \psi\zeta(1)]$ for the unstable kink mode discussed in Table 2 as a function of ψ for

several values of M in a finite-element expansion set. This representation is so good that in order to show anything we must scale out the dominant ψ behavior. Even so, the difference between ten and twenty elements cannot be seen on the figure.

Another useful way of viewing results is to present the spectrum as a function of the number of terms in the expansion. We do this in Fig. 2 for the system of Table 2. Note that, due to the truncation of the expansion functions, the continuous spectrum is approximated by a band of regularly distributed eigenvalues. This band fills in as the number of expansion functions is increased. It is interesting to observe how the ω^2's converge towards the limit points of the various continua branches. Analytic approximations to these limit points are clearly given by the relations $\omega_{\pm}^2 = \Omega^2/\rho_{\mp}$, where Ω^2 is an eigenvalue of the matrix T_o of Eq. (35) (see Fig. (1) of Dewar et al. [10]) and $\rho_{\mp}$ are the minimum and maximum densities within the plasma column. At M = 20 agreement to within one per cent is achieved between the analytic and computed limit points.

Another study of the efficacy of the code can be made by examining the eigenfunctions of the continuous spectrum in the vicinity of a singularity of the matrix T of Eq. (35). As shown in Eq. (47), the eigenfunctions should vary as $\xi_o \ln |\psi-\psi_s|$ where ψ_s is the location of the singularity and ξ_o is the associated eigenfunction of T_o. From this it can be deduced that the jumps in the derivatives of the different Fourier components (in θ) for the nonconstant density case should be proportional to the ratios of these components in the eigenfunction ζ_ℓ for the constant

density case. To test how well this is satisfied, we consider such a mode in the system of Table 2. Several components of a singular eigenfunction, determined by means of a finite-element expansion, are shown in Fig. 3 for this case. For the calculated eigenvalue the singularity should occur analytically at $\psi_s = 0.51$, and the derivatives can be approximated by differencing. A comparison of the numerical results with the analytical predictions for this case with M = 6 is given in Table III. An analogous result using the Fourier-Bessel expansion, is also given. The finite-element expansion provides a somewhat better description of the eigenfunctions. It is useful to observe that in general the agreement is improved as M is increased in the finite element technique (good accuracy is achieved with M = 10 as demonstrated in the last column of Table III), since increasing the value of M localizes the evaluation of the derivative closer to the surface where the $\ln|\psi-\psi_s|$ term is dominant. In the Fourier-Bessel treatment, however, extreme care must be taken to avoid truncation errors in the evaluation of the matrix elements as the number of expansion functions is increased, with the result that it is practically impossible to expect really good agreement with the theory for localized modes. This observation provides a strong argument for the use of a finite-element expansion.

To indicate how well the eigenfunctions can be represented by a finite-element expansion, we show in Fig. 4 the imaginary part of $\vec{\xi}\cdot\vec{\nabla}\psi$ for the configuration of Table 2.

SUMMARY

Here we have described the formalism for a numerical program to determine the complete spectrum of general axisymmetric toroidal configurations. We have applied it to a special simple model, for which analytic results are available,[10] in order to compare the efficacy of global versus local expansion techniques. Especially in the case where there are continuous spectra, the adoption of a finite-element expansion is shown to be superior.

ACKNOWLEDGEMENTS

The authors express particular gratitude to Drs. D. A. Baker, J. P. Friedberg, and B. M. Marder who gave freely of their experiences, preferences, and prejudices concerning various methods of approaching the problem. Discussions with F. Troyon and K. Appert were very valuable. Discussion with R. A. Anderssen concerning Galerkin's method were illuminating. We thank R. F. Kluge for programming assistance.

This work was supported by the U. S. Atomic Energy Commission, Contract AT(11-1)-3073; it utilized computer facilities provided in part by National Science Foundation Grant NSF-GP579.

REFERENCES

[1] G. KÜPPERS, D. PFIRSCH, AND H. TASSO, Plasma Physics and Controlled Nuclear Fusion Research (IAEA, Vienna, 1971) Vol. 2, page 529.

[2] T. TAKEDA, Y. SHIMOMURA, M. OHTA, AND M. YOSHIKAWA, Phys. Fluids 15, (1972), 2193

[3] J. P. FRIEDBERG AND B. M. MARDER, Phys. Fluids 16, (1973), 247.

[4] G. LAVAL, R. PELLAT, AND J. S. SOULE, Phys. Fluids 17, (1974), 835.

[5] D. A. BAKER AND L. W. MANN, Bull, Am. Phys. Soc. II 18, (1973), 1327.

[6] J. A. WESSON AND A. SYKES, Plasma Physics and Controlled Nuclear Fusion Research (IAEA, Vienna, 1974) IAEA-CN-33/A12-3.

[7] W. SCHNEIDER AND G. BATEMAN, Plasma Physics and Controlled Nuclear Fusion Research (IAEA, Vienna, 1974) IAEA-CN-33/A12-1.

[8] K. APPERT, D. BERGER, R. GRUBER, F. TROYON, AND J. RAPPAZ, ZAMP 25, (1974), 229.

[9] T. J. M. BOYD, G. A. GARDNER, AND L. R. T. GARDNER, Nucl. Fusion 13, (1973), 764.

[10] R. L. DEWAR, R. C. GRIMM, J. L. JOHNSON, E. A. FRIEMAN, J. M. GREENE, AND P. H. RUTHERFORD, Phys. Fluids 17, (1974) 930.

[11] J. TATTARONIS AND W. GROSSMAN, Proceedings of the Second Topical Conference on Pulsed High-Beta Plasmas (Garching, 1972) paper B5.

[12] H. WEITZNER, Phys. Fluids 16, (1973), 237.

[13] J. P. GOEDBLOED AND H. J. L. HAGEBEUK, Phys. Fluids 15, (1972), 1090.

[14] H. GRAD, Proc. Nat. Acad. Sci. 70, (1973), 3277.

[15] I. B. BERNSTEIN, E. A. FRIEMAN, M. D. KRUSKAL, AND R. M. KULSRUD, Proc. Roy. Soc. (London) A244, (1958), 17.

[16] L. V. KANTROWITZ AND V. I. KRYLOV, Approximate Methods of Higher Analysis (Interscience Publishers, Inc., New York, 1958).

[17] S. G. MIKHLIN, The Problem of the Minimum of a Quadratic Functional (Holden-Day, Inc., San Francisco, 1965), Sect. 11-13.

[18] S. G. MIKHLIN , The Numerical Performance of Variational Methods (Walters-Nordhoff Publishing Co., Groninger, The Netherlands, 1971), Ch. 7.

[19] J. P. FRIEDBERG AND F. A. HAAS, Phys. Fluids 17, (1974) 440.

[20] B. M. MARDER, Phys. Fluids 17, (1974), 634.

[21] D. A. BAKER. R. L. DEWAR, R. C. GRIMM, AND L. W. MANN, (to be published).

[22] M. S. CHANCE, R. L. DEWAR, A. H. GLASSER, J. M. GREENE, R. C. GRIMM, S. C. JARDIN, J. L. JOHNSON, B. ROSEN, G. V. SHEFFIELD, AND K. E. WEIMER, Plasma Physics and Controlled Nuclear Fusion Research (IAEA, Vienna) IAEA-CN-33/A12-4, (1974).

[23] K. APPERT, D. BERGER, AND R. GRUBER, Phys. Fluids 17, (1974) 1471.

[24] J. P. GOEDBLOED, H. GRAD, W. GROSSMANN, AND J. TATTARONIS, private communication.

Table I

M	ℓ=0 Alfvén		ℓ=2 Kink		ℓ=4 Kink	
	BF	FE	BF	FE	BF	FE
2	2.83555	2.85150	-0.552768	-0.552896	7.06215	7.19253
3	2.84768	"	-0.552870	"	7.29600	7.30292
4	2.85000	"	-0.552881	"	7.34408	7.33751
5	2.85076	"	-0.552892	"	7.36067	7.35274
6	2.85108	"	-0.552894	"	7.36800	7.36080
7	2.85124	"	-0.552895	"	7.37178	7.36558
8	2.85133	"	-0.552896	"	7.37393	7.36865
9	2.85138	"	-0.552896	"	7.37525	7.37074
10	2.85142	"	-0.552896	"	7.37610	7.37223
Exact	2.85150		-0.552896		7.37851	

Values of ω^2 for a constant density elliptic plasma column with a/b = 0.5. Estimates are given for both global (BF) and finite-element (FE) expansions as a function of the number (M) of expansion functions. Exact results from reference [10] are given for comparison. (64 bit precision)

Table II

ℓ= 2 Kink

M	BF	FE
2	-0.593664	-0.594428
3	-0.594632	-0.594793
4	-0.594872	-0.594921
5	-0.594953	-0.594985
6	-0.594980	-0.594993
7	-0.595010	-0.594980

Values of ω^2 for the case of Table I, but with parabolic density profile. (32 bit precision)

Table III

ℓ	$\Delta(\zeta'_\ell)$			
	Computed M=6		Theory	Computed M=10
	FE	BF		FE
-4	0.0035	0.0017	0.0045	0.0042
-2	-0.0209	-0.0168	-0.0213	-0.0210
0	0.1512	0.1312	0.1522	0.1444
2	1.0	1.0	1.0	1.0
4	-0.0465	-0.0271	-0.0584	-0.0553

Estimates of the jump in the derivative across the singular surface (ψ_s=0.51) of various Fourier components, evaluated using finite-element expansions, Bessel functions, and according to the theory of Section IV. Parameters for this case are the same as those of Table II. Computed results for both expansions were evaluated with a set of 6 expansion functions. Results with 10 finite elements are included for comparison.

Symbols used and page where they first occur:

ω	omega (l.c.)	p.5 above Eq. (1)
ξ	xi (l.c.)	" "
δ	delta (l.c.)	" Eq. (1)
τ	tau (l.c.)	p.6 Eq. (2)
ρ	rho (l.c.)	" "
$\int$	integral	" "
κ	kappa (l.c.)	" Eq. (3)
γ	gamma (l.c.)	" "
∇	del	" "
Φ	phi (u.c.)	" above Eq. (4)
Σ	summation [sigma (u.c.)]	" Eq. (4)
<>	this bracket must be kept inviolate with whatever is enclosed	" Eq. (5)
∞	infinity	" bottom line
ε	epsilon	P.7 line 4
ψ	psi (l.c.)	p.8 Eq. (6)
ϕ	phi (l.c.)	" "
Θ	theta (u.c.)	p.9 above Eq. (7)
∂	partial	" "
$\mathcal{J}$	script J	" Eq. (7)
π	pi (l.c.)	" "
ζ	zeta (l.c.)	p.10 Eq. (9)
χ	chi (l.c.)	" above Eq. (10)
ℓ	script L (l.c.)	p.11 Eq. (13)
Υ	upsilon (u.c.)	p.12 Eq. (16)
$\hat{M}$	M (u.c.) with caret	p.17 Eq. (24)

Symbols used and page where they first occur:

$\mathcal{L}$	script L (u.c.)	p.21 Eq. (34)
λ	lambda (l.c.)	p.22 Eq. (37)
σ	sigma (l.c.)	p.23 Eq. (40)
υ	upsilon (l.c.)	p.24 Eq. (43)
$\bar{\zeta}$	zeta (l.c.) with bar	" Eq. (45)
$\bar{\sigma}$	sigma (l.c.) with bar	" above Eq. (46)
Γ	gamma (u.c.)	P.25 Eq. (48)
Ω	omega (u.c.)	P.28 line 14
Δ	delta (u.c.)	table III

All vector quantities, denoted by a superscript $\rightarrow$,($\vec{\xi}$), should be set in bold face.

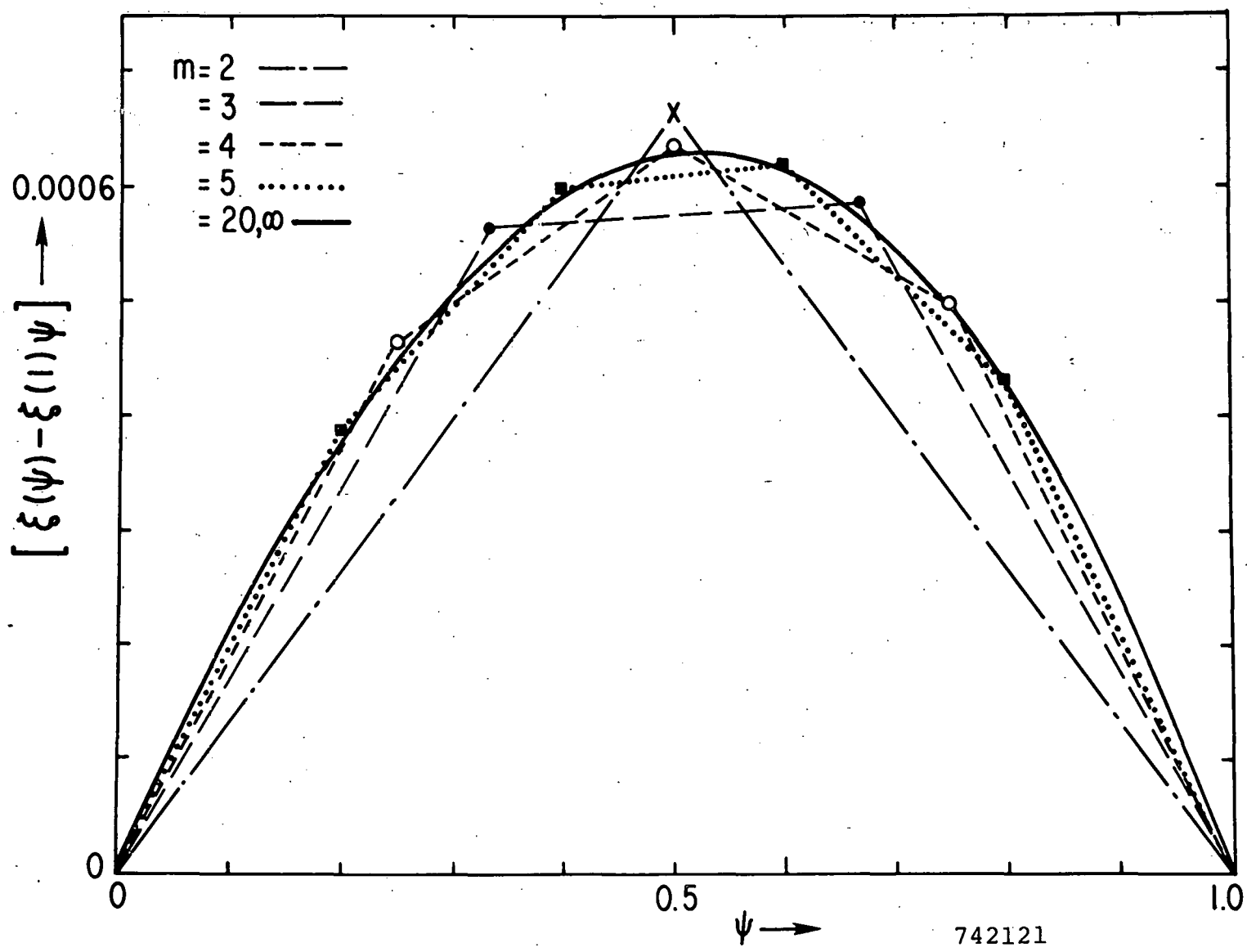

Fig. 1. The ℓ=2 component of $\zeta(\psi) - \psi\zeta(1)$ as a function of ψ in an elliptic plasma column with b/a = 2.0, q = 1.5, and ρ = 1.2 -0.4 ψ, showing rapidity of convergence as the number of finite elements is increased.

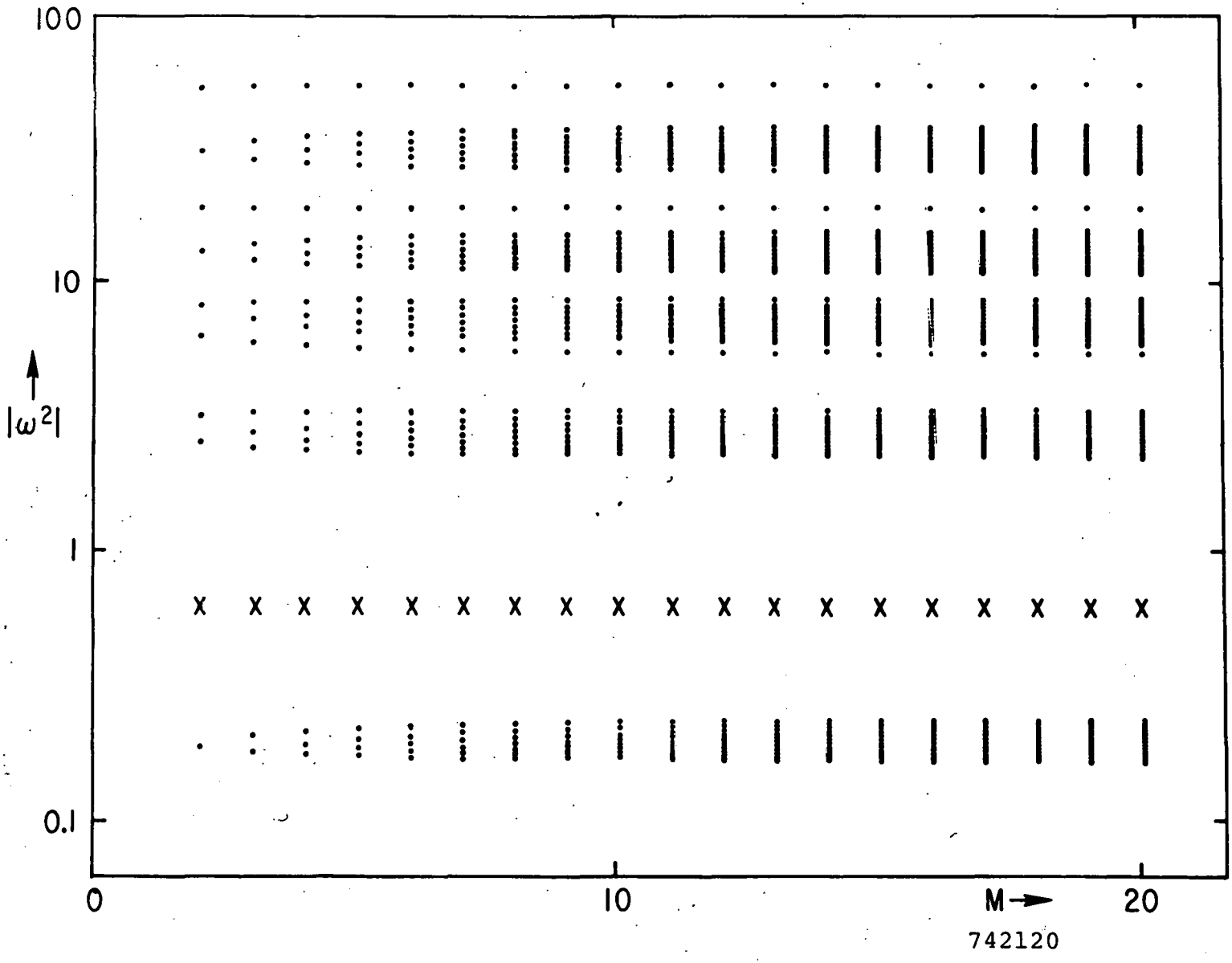

Fig. 2. Spectrum as a function of the number of finite elements for the configuration of Fig. 1. Note how quickly the continuous spectrum fills in as the number of elements is increased.

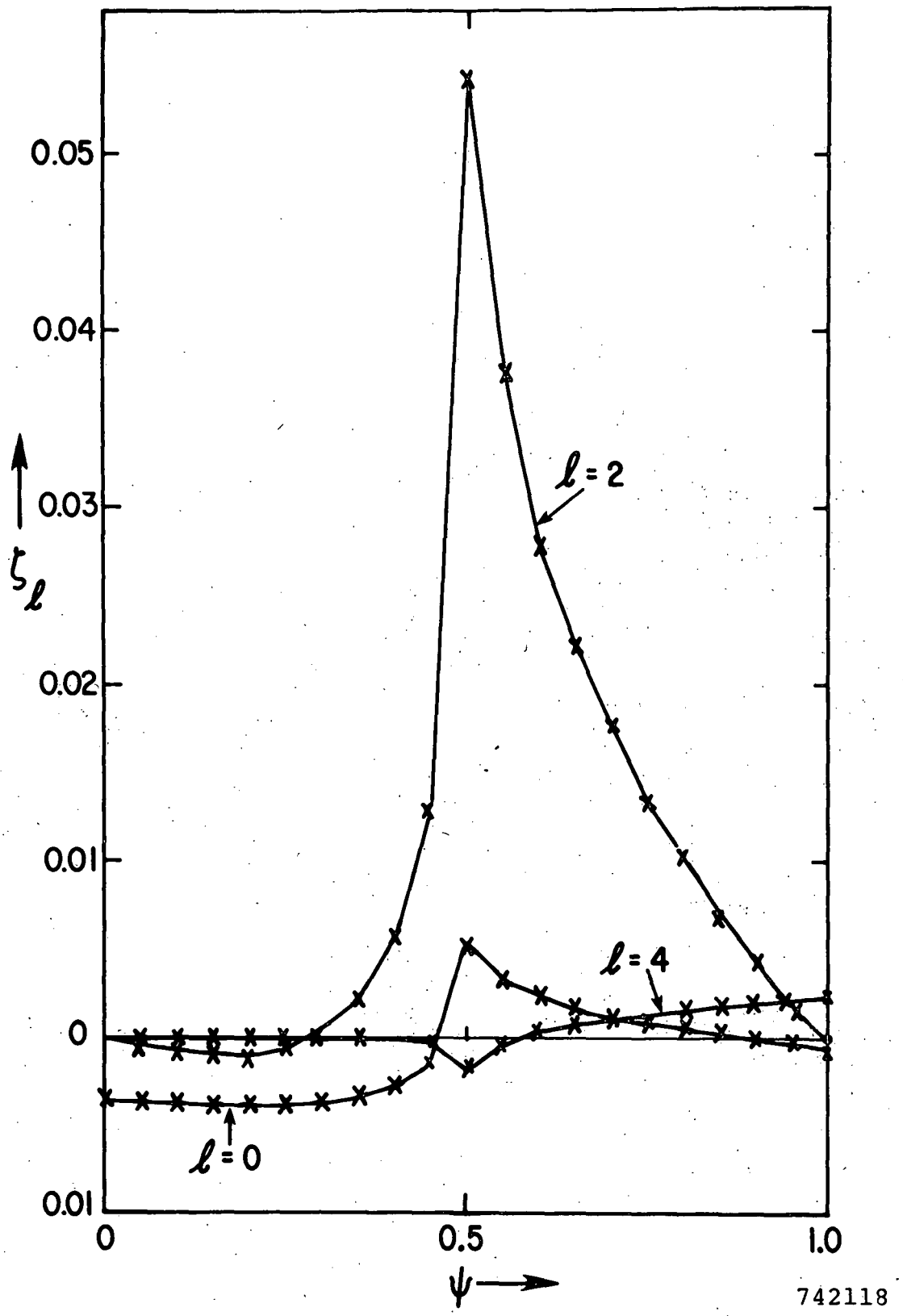

Fig. 3. The ℓ=0, 2, 4 components of ζ for a stable mode in the shear Alfvén continuum for the configuration of Fig. 1. The logarithmic singularity being studied occurs annalytically at ψ_s = 0.51.

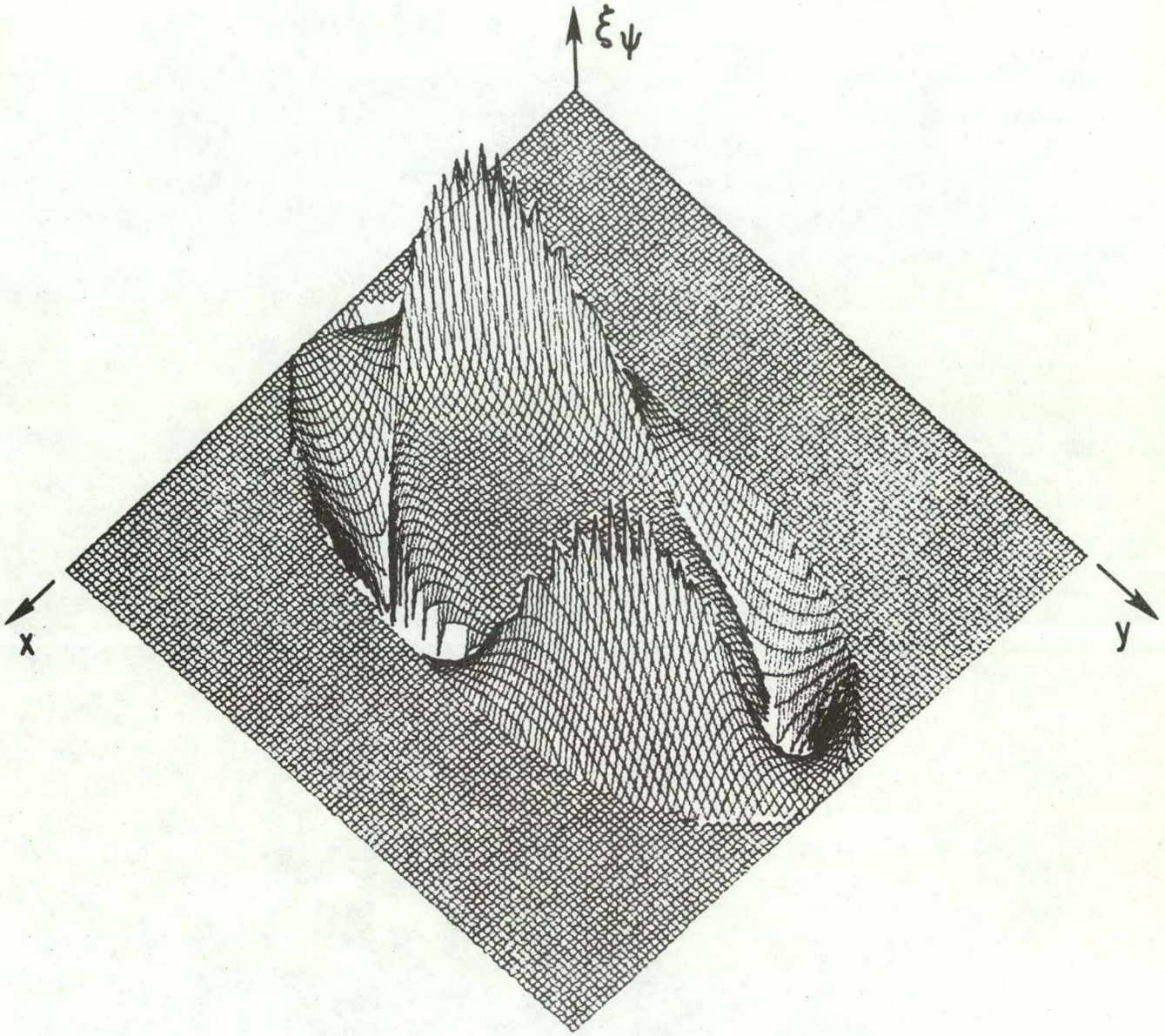

742123

Fig. 4. The imaginary part of $\vec{\xi}\cdot\vec{\nabla}\psi$ for the mode studied in Fig. 3 on a constant z surface such that ξ_ψ is largest at $\theta = \pi/4$.